



An Extended Active Learning Approach to Multiverse Analysis: Predictions of Latent Variables from Graph Theory Measures of the Human Connectome and Their Direct Replication^{*}

Daniel Kristanto, Carsten Gießing, Merle Marek, Changsong Zhou, Stefan Debener, Christiane Thiel, Andrea Hildebrandt[†]

Abstract

Multiverse analysis has been proposed as a powerful technique to disclose the large number of degrees of freedom in data preprocessing and analysis that strongly contribute to the current replication crisis in science. However, in the field of imaging neuroscience, where multidimensional, complex and noisy data are measured, multiverse analysis may be computationally infeasible. The number of possible forking paths given by different methodological decisions and analytical choices is immense. Recently, Dafflon et al. (2022) proposed an active learning approach as an alternative to exhaustively exploring all forking paths. Here, we aimed to extend their active learning pipeline by integrating latent underlying variables which are not directly observable. The extension to latent outcomes is particularly valuable for computational psychiatry and neurocognitive psychology, where latent traits are conceptualized as common cause of a variety of observable neural and behavioral symptoms. To illustrate our approach and to test its direct replicability, we analyzed the individual organization and topology of functional brain networks of two relatively large samples from the ABCD study dataset ($N = 1491$) and HCP dataset ($N = 833$). Graph-theoretical parameters that take into account both brain-wide and region-specific network properties were used as predictors of a latent variable reflecting general cognition. Our results demonstrate the ability of the extended method to selectively explore the multiverse when predicting a latent variable. First, the low-dimensional space created with the proposed approach was able to cluster the forking paths according to their similarity. Second, the active learning approach successfully estimated the prediction performance of all pipelines in both datasets. To interactively explore the multiverse of results, we developed a [Shiny app](#) to visualize the predictive accuracy resulting from each forking path and to illustrate the similarity between pipelines created by different combinations of data processing choice. The code for active learning and the app are available at the Github repository [ExtendedAL](#).

Keywords

Multiverse analysis, latent variable modeling, active learning, Shiny application.

Contents

Introduction	1
Methods	2
Brain Data	2
Behavioral Data	2
Multiverse Analysis Approach	3
An Active Learning Approach	3
Extension of the Method	3
The Multiverse of the Present Study	5
Implementation	6
Results	6
The search space from the proposed method	6
Active learning for guided multiverse analysis with SEM	6
Interactive visualization of multiverse outcome	7
Discussion	7
Conclusion	10
Acknowledgments	10
Code and Data Availability	12
Citation	12
References	12

Introduction

The large number of options available to researchers for preprocessing and analyzing their data has been cited as one of the reasons for the replication crisis in science (Paul et al. 2022). A huge heterogeneity in data analysis has recently been reported in cognitive neuroscience based on functional magnetic resonance imaging (fMRI) data (Botvinik-Nezer et al. 2020). The complexity arising from the nature of such data,

^{*}Presented 2023-10-09 with [DK slides](#) and [DK video](#) at [Guardians 2023](#)

[†]DK, CG, MM, SD, CT, and AH affiliated with University of Oldenburg; CZ with Hong Kong Baptist University; correspondence to [D Kristanto at Univ Oldenburg](#).

characterized by inherent noise and multidimensionality, requires extensive pre-processing to remove machine and physiological artefacts. It further offers many different ways to parameterize the properties of such multidimensional data. This means, for example, that there are many ways to define the characteristics of brain networks from fMRI time-series data, increasing the variability of research results.

Multiverse analysis has been proposed as a promising approach to address this problem (Steegen et al. 2016), because it allows researchers to systematically explore different analytical choices, called forking paths, and report the multiplicity of their findings. The primary goal of a multiverse analysis is thus to assess the robustness of research findings, thereby reducing the likelihood of false-positive discoveries and mitigating the replication crisis. However, performing multiverse analysis presents its own challenges, particularly in network neuroscience, which deals with high-dimensional fMRI data and where the number of forking paths can be excessive (Dafflon et al. 2022; Botvinik-Nezer et al. 2020).

Recently, Dafflon and colleagues (2022) proposed an active learning-based approach to estimate the outcomes of multiple forking paths without the need for exhaustive computation of the multiverse (Dafflon et al. 2022). Their algorithm uses Bayesian optimization to sample a subset of forking paths and manually compute their outcome, and it uses Gaussian processes to estimate the outcome of the remainder. Dafflon et al.'s (2022) work applied this active learning approach to 1) predict brain age and 2) classify individuals with autism, using graph measures derived from fMRI-based whole brain networks. Both of these supervised learning problems are concerned with predicting an observed outcome variable.

However, in computational psychiatry and neurocognitive psychology, many outcome variables of interest cannot be measured directly and therefore reflect "latent" variables. To facilitate multiverse analyses in these fields, we extended Dafflon et al.'s (2022) active learning-based approach in two key ways. First, we augmented the approach with a predictive model that includes an endogenous variable that is latent and can be indicated by quantitative or ordinal measures. To accomplish this, we combined the proposed method by Dafflon et al. (2022) with Structural Equation Modeling (SEM, with latent variables) to infer predictive accuracy of brain measures with respect to a latent variable.

The original study by Dafflon used active learning to infer the prediction performance of each forking path without exhaustively sampling each of them. In short, active learning is an approach in machine learning where the model, during learning, can select the data that need to be labeled with the desired output (Settles 2009). SEM is a statistical analysis tool used to model the relationships between observed and latent variables (Kline 2015). In this study, the latent, non-directly measurable variable is general cognition g , which is estimated from various directly observable measures of performance on cognitive tasks (e.g., memory, reasoning and processing speed). In 1904, Spearman found that all indicators of cognition were positively correlated, referred to as the positive manifold, which is interpreted as general intelligence g (Spearman 1904). Recent studies have found that g is strongly associated with school achievement (for a review see Kriegbaum et al. 2018). Given the importance of g , a growing body of research in neuroscience has investigated the neural basis of g from the perspective of neurons (Bruton 2021), brain areas' activation patterns (Kovacs and Conway 2016; Jung and Haier 2007), and more recently, brain networks (Barbey 2018; Barabási et al. 2023).

In addition to combining Dafflon's method with SEM, we propose an

alternative approach to estimating forking path (pipeline) similarity that incorporates both brain-wide and region-specific graph measures. Note that the approach proposed by Dafflon et al. (2022) is only applicable to region-specific graph measures. Importantly, global graph measures, such as global efficiency and modularity, are relevant to predict behavioral outcomes in many applications (Alavash et al. 2015). To assess the effectiveness of our extended multiverse analysis approach and to test its direct replicability across datasets, we conducted a study on two large samples of NABCD = 1491 individuals from ABCD study and NHPC = 833 from HCP study (see Materials for the details of the datasets). Moreover, to better and more dynamically explore the multitude of results, we created an interactive visualization of the multiplicity of outcomes resulting from an exhaustive multiverse analysis using the Shiny app platform. The corresponding code is openly available at the Github repository [ExtendedAL](#).

Methods

We illustrate and test our multiverse analysis approach to predicting a latent outcome variable by examining the relationship between graph measures of the functional human connectome and g . We use data from two open-access studies. The first dataset was derived from the Adolescent Brain Cognitive Development (ABCD) study, the largest shared neuroimaging dataset to date. In order to obtain both brain and behavioral data, we used the ABCD data release 2.0.1. The second dataset was obtained from the Human Connectome Project (HCP) Young-Adult study.

Brain Data

Functional connectivity (FC) between brain regions was analyzed using functional magnetic resonance imaging (fMRI) data. Specifically, the blood oxygenation level dependent (BOLD) time series of different brain regions were measured as an indicator of underlying neuronal activations. The pairwise correlations between BOLD time series were calculated as an estimator of functional brain connectivity. For the ABCD dataset, we used previously preprocessed resting-state fMRI data (J. Chen et al. 2022) available at [NDA repository](#). Mean BOLD time series across voxels were extracted from a total of 419 brain regions, 400 cortical regions of interest (ROIs) from Schaefer's atlas (Schaefer et al. 2018) and 19 subcortical ROIs (Fischl et al. 2002). We computed the pairwise correlations between time series which resulted in functional connectivity matrices (419 x 419 brain areas) for 1491 individuals. The data have been preprocessed to remove motion-related, machine-related, and physiological noise (see J. Chen et al. 2022 for details). For the HCP dataset, we used data from our previously published study with NHPC = 833 individuals (Kristanto et al. 2023). In contrast to the ABCD dataset, time series of 360 brain regions were extracted according to the multimodal parcellation atlas and functional connectivity matrices with a dimensionality of 360 x 360 were calculated (Glasser, Coalson, et al. 2016). The MR data were also cleaned from artifacts using a minimal preprocessing pipeline from HCP (Glasser, Sotiropoulos, et al. 2013).

Behavioral Data

The aim of the present analysis was to explore the relationship between graph measures and a latent variable of general cognition, g . We used performance scores of five behavioral tasks available in both ABCD and HCP datasets: Picture Vocabulary (PicVocab), List Sorting Memory (ListSort), Pattern Comparison (PattComp), Picture Sequence (PicSeq),

and Reading Comprehension (Reading) (Fig. 1B). Picture Vocabulary and Reading Comprehension are known as indicators of crystallized intelligence, List Sorting memory is an indicator of reasoning ability, Pattern Comparison is an indicator of processing speed ability, and Picture Sequence is an indicator of memory.

All the tasks are part of the National Institute of Health Toolbox Cognition Battery NIH Toolbox. The details of the behavioral tasks are available from Casey et al. 2018 for ABCD dataset and Barch et al. 2009 for HCP dataset.

Multiverse Analysis Approach

Since the goal of this study is to extend a previously proposed method, in this section we first briefly describe the published method and point out the aspects that we aim to extend. Second, we explain our proposals for extending the aspects we point out from the original study. Third, we explain the design of our multiverse analysis and finally, we briefly explain the implementation of the extended method.

An Active Learning Approach

An active learning-based method for exploring the results in a multiverse analysis of predicting observed age of individuals from brain-based graph measures has been recently proposed (Dafflon et al. 2022). This method aims to estimate the analysis results (e.g., prediction performance) from a series of possible forking paths (544 and 384 forking paths in total for age prediction and autism classification, respectively) by sampling only a small fraction of them and inferring the other forking paths. The approach has been shown to be comparable to an exhaustive analysis, where each fork is executed sequentially to obtain the prediction.

Dafflon's et al. active learning approach for multiverse analysis consists of several steps. The first step is to prepare the brain and behavioral data and partition them into three sets. The first dataset is used to create the low dimensional space for embedding the similarity of graph measures obtained by all forking paths. The second dataset is used for prediction/classification, and the third dataset is for evaluation, thus to assess the performance of the best pipelines identified by active learning.

In the second step of the multiverse analysis method an embedding into a two-dimensional space of the forking path is created based on the similarity of the graph measures obtained by each forking path. This step is performed in the first dataset. In detail, the output of each forking path is a vector containing a graph measure of all brain regions. To obtain the forking paths' similarity, the cosine similarity of these vectors between any two individuals is computed, resulting in a similarity matrix of $(N) \times ((N)-1)/2 \times (NF)$, where (N) is the number of individuals and (NF) is the number of forking paths (for a detailed illustration, please refer to Fig. 8 of the original article (Dafflon et al. 2022)). Note that this step requires a vector as the output of all forking paths and is, therefore only applicable to region-specific graph measures. Next, the matrix is submitted to a dimension reduction algorithm to obtain a two-dimensional space of forking paths' similarity, which we refer to as the "search space" with the dimension of $2 \times (NF)$.

The third step – which aims at method evaluation – is to perform an exhaustive analysis to obtain a "true prediction accuracy" of each forking path. This step is performed on the second dataset. In the case of age prediction, this is done by predicting the age from the graph measures as the output of each forking path. The end result of this step is a vector of the true prediction accuracy of each forking path (e.g.,

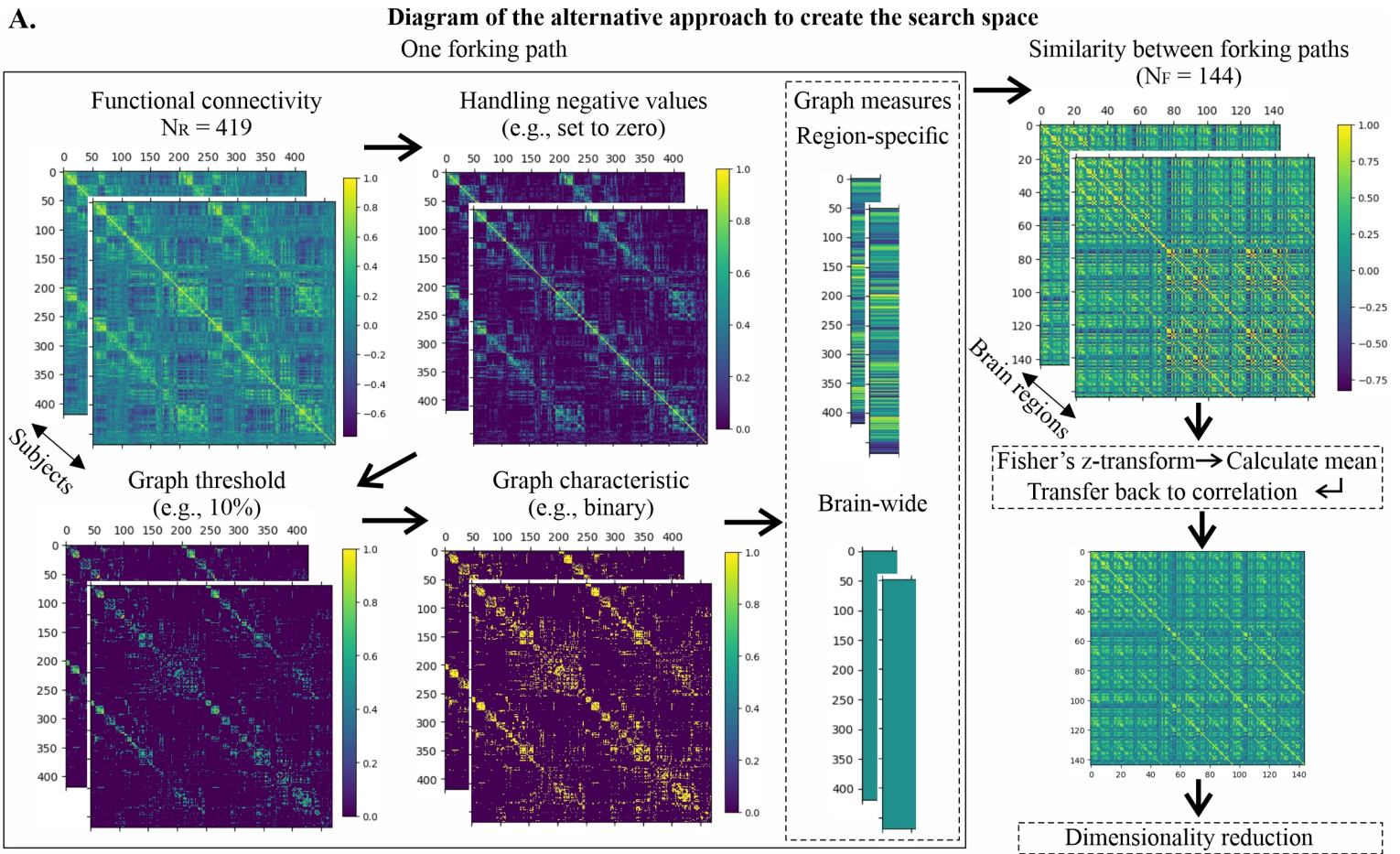
evaluated by the mean absolute error between predicted and actual age).

Finally, an active learning algorithm based on Bayesian optimization and Gaussian processes is implemented in the search space to infer the prediction accuracy of each forking path and to compare it with the true prediction accuracy obtained from the exhaustive search. The search space is a 2-dimensional space where the forking paths are represented as points in the space. The active learning first performs a burn-in phase where it randomly selects 10 points and evaluates their prediction accuracy. After this phase, more points (i.e., 40 points) are selected using Bayesian optimization and the prediction accuracy of those points is evaluated by predicting an observed outcome variable (age in the application) using graph measures derived from the corresponding forking paths. Finally, the Gaussian process is implemented to estimate the prediction accuracy of the other points/forking paths based on the selected points.

To test the robustness of the active learning, the whole analysis is repeated 20 times, each with different starting points. The third dataset is finally used to evaluate the prediction performance of the best pipeline identified by the active learning in different repetitions. However, we emphasize that here we are interested in using the active learning to estimate the prediction performance of all possible forking paths and in reporting the results from all forking paths.

Extension of the Method

Developing the search space that handles both brain-wide and region-specific graph measures: As a first extension, we proposed a different approach to generating the search space that allows the use of brain-wide and region-specific graph measures. Specifically, the use of brain-wide graph measures is in line with the current trend in behavioral neuroscience that aims to associate a measure from the whole brain to more general abilities such as g . It is important to note that the search space is the low-dimensional representation of the similarity (or dissimilarity) matrix between the forking paths. In the original study, the cosine similarity of the graph measures for the brain regions between all possible pairs of individuals was used to define the matrix. However, this approach is not applicable when the output of the forking path is a single value, which is the case for the brain-wide graph measures (e.g., global efficiency and modularity). The cosine similarity between two single values is always 1 ($\cos 180^\circ$) because they overlap and are on the same line. Therefore, no matter how much the forking paths differ when computing the brain-wide graph measures, the cosine similarity will always be 1 for any given pair of individuals. Notably, the absolute differences and mean absolute differences can also be used to replace cosine similarity, since they can handle graph measures with single and multiple values. However, since we include the options of graph measures in the forking paths, and thus different forking paths can have different graph measures, using (mean) absolute difference may not work when comparing forking paths with different graph measures. To overcome this challenge, we propose a different approach to construct the search space from the similarity matrix of the forking paths with brain-wide and region-specific graph measures, as shown in Fig. 1A. In detail, performing the analysis on the left side of Fig. 1A (all steps within the black box) for all forking paths results in a 3-dimensional matrix of size $(NF) \times (N) \times (NR)$, where (NF) is the number of forking paths, (N) is the number of subjects, and (NR) is the number of brain regions. Next, the similarity between a pair of forking paths is calculated for each brain region (right side of Fig. 1A). This is done by computing the



B. Diagram of the SEM for predicting general intelligence (g)

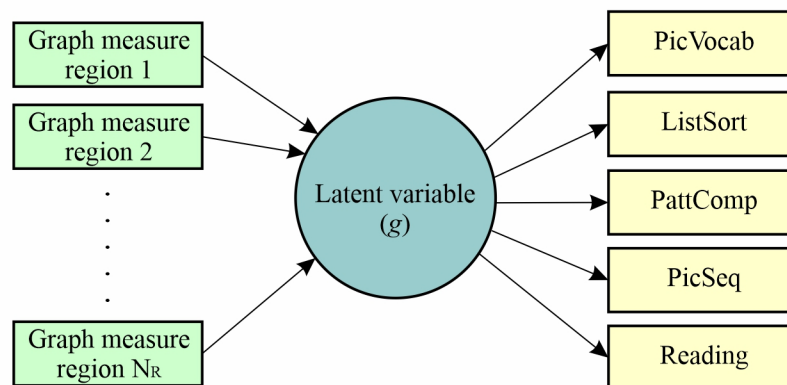


Figure 1: (A) Illustration of an alternative approach that handles both brain-wide and region-specific graph measures to create the search space. (B) A diagram of the SEM for predicting general cognition (g).

Pearson's correlation coefficient between two graph measure vectors of two forking paths in each brain region across individuals. The correlation coefficient fills the cells in the matrix at the top right of Fig. 1A. There are (NR) matrices, where each matrix has the size of $(NF) \times (NF)$. Importantly, the differences between forking paths with brain-wide and region-specific brain measures appear in these matrices of $(NF) \times (NF)$. Note that columns and rows represent forking paths. For the cells with both column and row representing forking paths with brain-wide graph measures, the values are identical across brain regions ((NR)) since the brain-wide graph measures do not vary across regions. In contrast, for the cells with column and/or row representing forking paths with region-specific graph measures, the values are different across brain regions since the graph measures are different across regions. Next, the average of these matrices across brain regions is computed by first transforming them using Fisher's z-transformation to account for the nonlinearity of the correlation coefficients (Silver and Dunlap 1987). Notably, the averaging only affects the cells containing forking paths with region-specific graph measures, but not the forking paths with brain-wide graph measures, since the values are identical across brain regions. The averaged matrix is transformed back into a correlation matrix before being subjected to the dimension reduction approach to obtain the search space of size $2 \times (NF)$.

In particular, a step to reduce the dimension (i.e., number of features) of each forking path is a key step to perform the active learning algorithm with small number of observations (i.e., 144 forking paths). The step allows the creation of a low-dimensional search space for the active learning. Using the similarity matrix (with a size of 144×144 , where 144 is the number of forking paths) as the active learning search space will require much more observations/forking paths which are distributed across space in order to implement the active learning, since each forking path will have 144 features or dimensions. Here, we showed that, although we reduced the number of dimensions, the results of the search space in the lower 144×2 space, still retains the information related to the similarity between forking paths, where similar forking paths are located close to each other. In addition, we also found that the search space with only two dimensions allows active learning to mimic the results of the exhaustive search where we computed the performance of each forking path (see Results).

Integrating active learning approach with SEM: The second extension of the multiverse analysis proposed here involves integrating the SEM model with active learning to infer the explained variance of a latent outcome variable from graph measures. Unlike the method in the original multiverse analysis (Botvinik-Nezer et al. 2020) which used only observed variables, the extension allows for inferring latent outcome variables commonly of interest in computational psychiatry and neurocognitive psychology. To do so, we replace the prediction model with SEM implemented using the *semopy* package (Igolkina and Meshcheryakov 2020; Meshcheryakov et al. 2021). The predictive performance of each forking path is evaluated by the explained variance of the latent variable from graph measures. Therefore, the exhaustive search will output a "true prediction accuracy" vector, which is indicated by the explained variance of each forking path. Active learning is then performed to infer this value. Fig. 1B shows a schematic of the SEM used in the present study to evaluate the proposed approach. The latent variable reflects general cognition, indicated by 5 items behavioral measures (see Materials). The latent variable is then predicted by graph measures of the connectome as described above. The explained variance of the latent variable becomes the predictive performance of each forking

path.

Interactive visualization of the multiverse analysis results: An interactive visualization of the results of all forking paths is the final extension of the multiverse analysis approach proposed here. For this we used the *Shiny* package (Chang et al. 2023) in R the software for statistical computing (R Core Team 2021). A graph visualization based on force network *networkD3* package (Allaire et al. 2022) was created to represent the multiverse where the nodes are the forking paths and the edges are the relationships between the forking paths. Notably, we set the node size to represent the prediction performance of the corresponding forking path. A larger node indicates that the corresponding forking path has higher prediction performance. Moreover, the relationship between forking paths is represented by the similarity between them, which was taken from the matrix of average similarity between forking paths (Fig. 1A). We also added some features to the shiny application. First, hovering the mouse over the nodes will trigger the name of the forking paths and all other connected forking paths. Clicking on a node brings up a dialog box with the corresponding forking path and its prediction performance. Hovering over the edges will show the degree of similarity between connected forking paths. Finally, we also incorporated some option buttons where the user can select a specific forking path and explore other paths connected to it. In addition, a slider option allows users to specify the threshold of similarity between forking paths (e.g., to find the forking paths that are connected by a correlation coefficient of at least 0.8).

The Multiverse of the Present Study

In this study, a multiverse analysis was performed in which a latent variable of g was predicted from graph measures derived from fMRI data. First, the investigated forking paths were identified through a systematic literature review on the multiverse of fMRI data preprocessing and fMRI graph analysis steps (paper in preparation). This multiverse covers a wide range of pre-processing and analysis steps in fMRI-based graph analysis including structural image pre-processing, functional image preprocessing, noise/artifact removal, functional connectivity definition, and network definition. In this study, we focus only on the small fraction of pre-processing paths which we call data multiverse. Analysis paths were pre-dominantly selected if the corresponding options are variable across studies and are highly controversial:

- *Paths for handling negative correlations:* Use absolute values, keep negative values, assign 0 values to the negative values, discussed in G. Chen et al. 2011;
- *Paths for Controlling graph sparsity:* 50%, 30%, and 10%, discussed in Franco 2022. Notably, these options cover a variety of network sparseness where '50%' represents a relatively dense network, while 10% represents a sparse network with only 10 percent of all possible connections;
- *Paths for defining graph edges:* weighted and binarized, discussed in Xiang et al. 2020;
- *Paths for computing graph measures:* strength, betweenness centrality, clustering coefficient, eigenvector centrality, local efficiency, global efficiency, modularity, and participation coefficient. for detail of each measure please refer to Brain Connectivity Toolbox (Rubinov et al. 2009).

In total, there are $3 \times 3 \times 2 \times 8 = 144$ different forking paths. Note that modularity, global efficiency, and participation coefficient are brain-wide graph measures, while the rest are region-specific graph measures.

Implementation

Overall, the implementation of the proposed method is similar to the original study. In the first step we divided the data into 3 sets by keeping the similar ratio of the original study (seimilar number for set 1 and set 3, and higher number for set 2). Since we had a larger sample size in both datasets than the original study, for ABCD dataset, we used 350 individuals to define the search space, 791 individuals to perform the prediction based on the SEM, and 350 individuals to validate the best-performing forking paths identified by active learning. We kept the ratio for the HCP dataset: 200 individuals to define the search space, 433 individuals to perform the prediction based on the SEM, and 200 individuals to validate the best-performing forking paths identified by active learning. Notably, we are more interested in reporting the results from all possible forking paths and not in finding the best-performing forking paths. The validation here further confirms the robustness of the results obtained by active learning from different repetitions using different forking paths in burn-in/initialization phase.

To create the search space, we followed the pipeline shown in Fig. 1A. In line with the result of the original study, we applied multidimensional scaling (MDS) as a dimension reduction method, because this embedding approach was shown to perform best in Dafflon et al. 2022. Further embedding methods can be explored in the future. The exhaustive search was then performed to obtain the "true prediction performance" vector of the explained variance of the latent variable for all forking paths. Notably, for the SEM model to predict the latent variable by the graph measures, we only used the brain areas in dorsal attention and fronto-parietal networks (Schaefer et al. 2018; Yeo et al. 2011). The areas of these networks were found to be associated with g (Jung and Haier 2007; Hilger et al. 2020). In total, we have 77 and 89 brain areas for the ABCD and the HCP datasets, respectively, to predict g . Active learning was then performed to quantify the explained variance in the latent variable, which was further compared with the result of the exhaustive search. Since we had a smaller number of pipelines as compared with the original study, we used different numbers of forking paths to train the active learning (i.e., 10 points randomly selected for the burn-in phase and 20 points selected using Bayesian optimization). We set the active learning to be exploratory, with a kappa of 10, following the result of the original study. We also run the active learning 20 times with different starting points to evaluate its robustness. For each iteration, we identified the best performing forking path. The robustness is indicated by the replicated best-performing forking paths identified across repetitions. Finally, we used the third dataset to validate the prediction performance of those best-performing forking paths.

Results

The search space from the proposed method

The first result of the present study was the creation of a low-dimensional space (search space) by using the newly proposed approach to deal with both brain-wide and region-specific brain measures. As described in the original study (Botvinik-Nezer et al. 2020), the creation of the search space mainly aims to capture the similarity of the forking paths in the 2-dimensional space with the constraint that similar forking paths should stay close to each other.

The search space generated by our proposed approach shows that the forking paths are well distributed in the space, as shown in Fig. 2 for both datasets. More importantly, there is considerable structure in the location of the different forking paths, meaning that especially the similar types of graph measures, illustrated by different shapes, are generally proximal. Moreover, we see a clear distinction between the forking paths calculating graph measures related to integration (e.g., global efficiency and participation coefficient) versus segregation (e.g., modularity and local efficiency). This observation is true for both data sets. For the ABCD dataset (Fig. 2A), the forking paths of the integration graph measures are mostly located in the upper right part of the space, while the forking paths of the segregation graph measures are mostly located in the lower left part of the space. For the HCP dataset (Fig. 2B), the forking paths of integration graph measures are mostly located in the upper part of the space, while the forking paths of segregation graph measures are mostly located in the lower part of the space. This finding suggests that in both dataset, the proposed method to create a two-dimensional search space, was able to cluster the forking paths according to their similarity. In order to assess the similarity between the spaces from both datasets, we performed clustering analysis in the low-dimensional spaces from both datasets and computed the Rand Index ((RI)) of the clustering results, which is the ratio between the number of matching pairs and the number of pairs (Hubert and Arabie 1985). The (RI) value of '0' indicates that two clustering results are completely different, while a value closer to '1' represents high agreement between two clusterings. We defined the optimal number of clusters using the Elbow method based on the intra-cluster sum of squares, also known as inertia (Thorndike 1953). For both datasets, we found that the optimal number of clusters is 3. An (RI) value of 0.71 was determined for these three clusters, indicating that the clustering results in the low-dimensional spaces of the two data sets were very similar.

Given these results, first we conclude that the proposed similarity evaluation approach is suitable to create a low-dimensional space that serves as the search space for active learning where similar forking paths tend to be close to each other. Second, we found that the proposed approach can be replicated in a different dataset in terms of clustering results from the low-dimensional space. It is also important to note that the slight differences in terms of clustering results from the low-dimensional space between the data sets may be due to the differences in terms of the number of individuals available to create the low-dimensional space and the number of nodes in the FC (419 and 360 nodes for ABCD and HCP datasets, respectively).

Active learning for guided multiverse analysis with SEM

We implemented the proposed extensions of the guided multiverse analysis on the ABCD study and HCP datasets to predict the latent variable reflecting g using graph measures from fMRI data. The results are shown in Fig. 3. First, Fig. 3A captures the prediction performance of all forking paths when the exhaustive search (i.e., manual execution of all forking paths) was performed, left panel is for ABCD dataset and right panel is for HCP dataset. It can be seen that region-specific graph measures outperform brain-wide graph measures in explaining the variance of the latent variable. The prediction performance shown in Fig. 3A serves as the "true prediction performance" to be used to evaluate the performance of the active learning to guide the multiverse analysis.

Next, Fig. 3B shows how active learning selects the training points (=forking paths) in 5, 10, 15, 20, and 30 iterations and infers the predic-

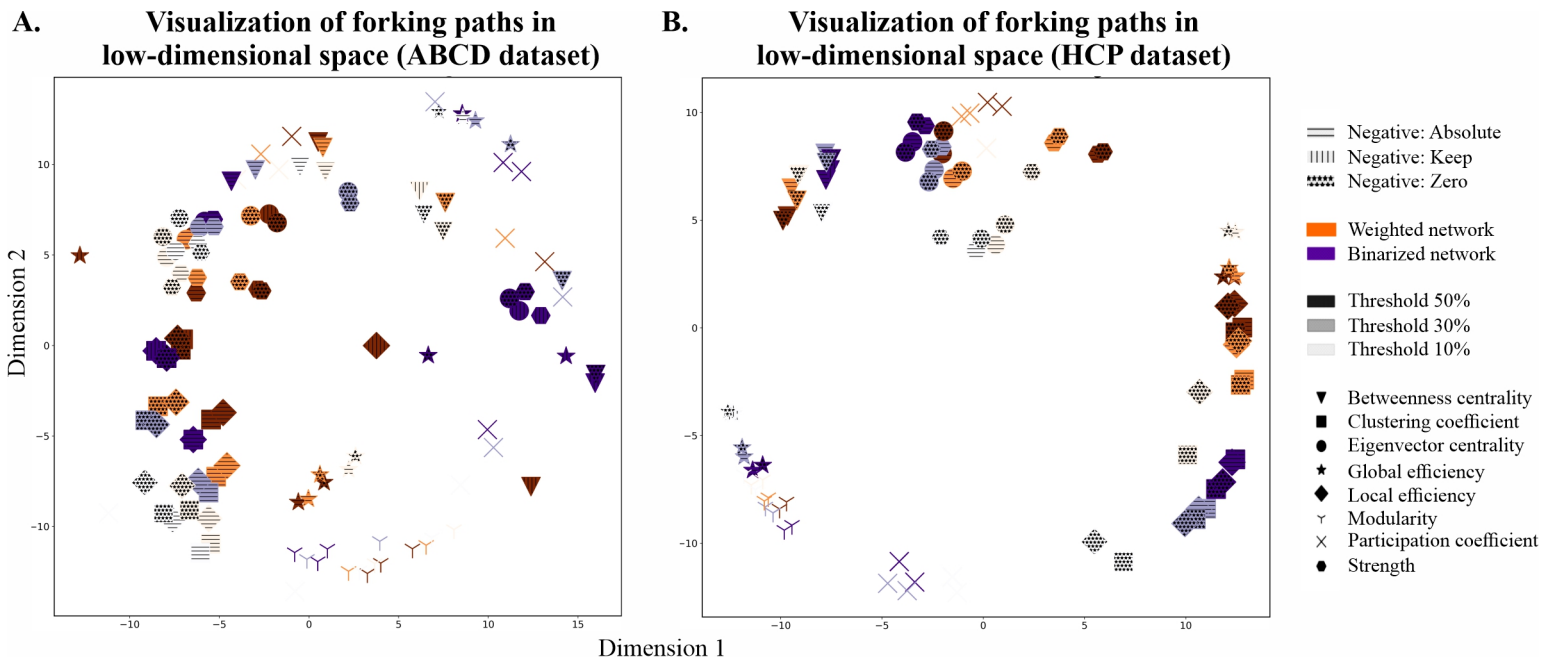


Figure 2: The visualization of forking paths in low-dimensional space for the ABCD dataset (A) vs. the HCP dataset (B). The items with different features (i.e. texture, color, shade, and symbols) represent the forking paths (NF = 144) in two dimensional space (see Methods).

tion performance of the search space in different iterations, left panel is for ABCD dataset and right panel is for HCP dataset. After 30 iterations (e.g., 30 training forking paths are selected), the active learning can satisfactorily mimic the prediction performance of all the forking paths from the exhaustive search. Notably, the Spearman correlations of the prediction performance of all forking paths between exhaustive search and active learning are 0.69 and 0.75 for ABCD and HCP datasets, respectively. This shows that the rank orders of the forking paths in terms of prediction performance obtained by exhaustive search and active learning are sufficiently similar. Next, we ran the active learning over 20 repetitions, where each repetition randomly selects different training points. Fig. 4 shows the comparison of prediction performance between exhaustive search and active learning across repetitions in the ABCD (Fig. 4A) and the HCP (Fig. 4B) datasets. The figures on the left panel are line plot of the Mean Absolute Error (MAE) of the prediction performance (explained variance of g) between the active learning and exhaustive search in 20 repetitions with different points for training. For both datasets, we found the MAE is around 0.05 for all repetitions. The figures on the right panel show the distribution of Spearman correlations of the prediction performance of all forking paths between exhaustive search and active learning across 20 repetitions. The correlations, which range from 0.37 to 0.75 for ABCD dataset, and from 0.58 to 0.77 for HCP dataset, indicate that active learning robustly mimics the prediction performance of all forking paths obtained from exhaustive search. The robustness of the active learning is also supported by the identification of similar best-performing forking paths across 20 repetitions. For the ABCD dataset the best-performing forking path is the following: keep the negative correlations, use a sparse network with a threshold of 10%, use a weighted network, and compute local efficiency as the graph measure. The analysis on HCP dataset identified a similar best-performing forking path across 20 repetitions: keep the negative correlations or set them to zero, use a sparse network with a threshold of 10%, use a weighted network, and compute either local

efficiency or betweenness centrality as the graph measures.

Interactive visualization of multiverse outcome

A screenshot of the interactive application (available online at <https://meteor-oldenburg.shinyapps.io/ExtendedAL/>) is shown in Fig. 5. Note that the results displayed in the interactive visualization originated from the ABCD dataset. When the threshold for the relationship (similarity, right bottom matrix in Fig. 1) between the forking paths is set to a higher threshold (e.g., 0.7), the clusters of the forking paths are shown based on the corresponding graph measures. Consistent with the search space discovery, the interactive visualization also shows that the similar forking paths (e.g. with similar graph measures) are highly correlated (connected) with each other. The user can also explore different thresholds to investigate the relationships between the forking paths. Moreover, the user can also select a particular forking path to explore how it is connected to other forking paths. For example, as also illustrated in the red box in Fig. 5, selecting the “betweenness centrality weighted 0.1abs” forking path will show the other forking paths that are connected to it.

Discussion

The present study has extended a previously proposed method for a guided multiverse analysis of fMRI based graph theory measures to predict behavioral outcomes (Dafflon et al. 2022). We show that our extensions perform well, allowing the use of both brain-wide and region-based graph measures and the prediction of latent variables from fMRI-based graph measures. In addition, since our goal is to report on the multiplicity of findings, we propose an interactive visualization of the results of the multiverse analysis, where the user can explore the outcomes obtained by all possible forking paths.

We first discuss the methodological contribution of the present study. The originally proposed method (Dafflon et al. 2022) is a valuable contribution to research when it comes to addressing the issue of the

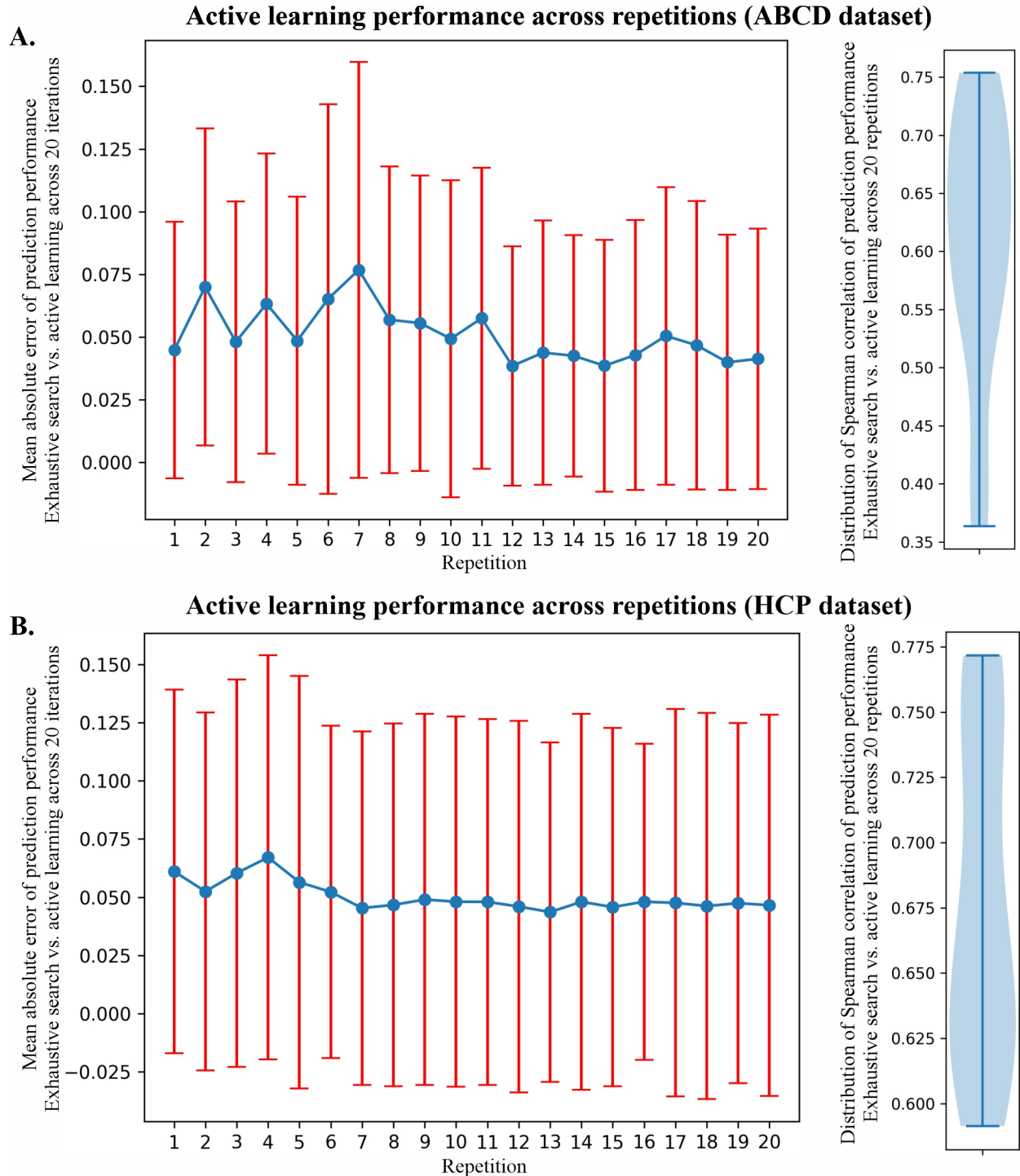


Figure 4: Prediction performance of active learning compared to exhaustive search across different repetitions for ABCD dataset (A) and HCP dataset (B). The left panel is the mean absolute error of prediction performance (explained variance of g) of all forking paths obtained by active learning and exhaustive search across repetitions. The right panel is the distribution of the Spearman correlations between the prediction performance of all forking paths obtained by exhaustive search and those from active learning across repetitions.

researcher's degree of freedom, as it provides an efficient method to explore the multiverse of possible decisions in a guided, well informed way. In line with this goal, we believe that this method can be further extended to target a larger user community by adding more flexibility and multiple features to it. Here, we added flexibility by allowing the combination of brain-wide and region-specific graph measures and added further modelling capabilities by integrating SEM as a predictive model to explain a latent outcome variable. Next, we also emphasize that the end product of this guided active learning method is not only to identify the best performing forking paths, but also to provide a full report of all possible forking paths and to gain knowledge about the sensitivity of the results with respect to the decisions of different researchers. In this sense, we introduced an interactive Shiny application to visualize not only the results of all forking paths, but also how the forking paths are related to each other in terms of similarity between the graph measures obtained.

Second, we now discuss possible future applications building upon the results of our study. Note that we predicted the latent variable using only a subset of brain areas related to cognitive control and risk-taking behaviors, and thus did not apply any regularization within the prediction model. A future study may include more predictors, such as areas from the whole brain, and apply regularization in the prediction model aiming to extract the important brain areas for prediction. We noticed that regularization options are also available in the *semopy* package (Meshcheryakov et al. 2021) which can be explored in the future. Relatedly, other features in *semopy* can also be explored to elaborate on more advanced SEM models which are potentially relevant to test brain-behavior associations. Furthermore, the forking paths we use in this study are also limited to data processing steps after functional connectivity definition. Follow-up studies may also consider additional forking paths related to fMRI data preprocessing in spatial or temporal domains, especially those dealing with noise removal. For these preprocessing decisions, a slightly different choice may contribute to significantly different results. In addition, other forking paths may be found beyond the data pre-processing domain or data multiverse. For example, one could consider different ways to compute the similarity matrix across forking paths and whether the Fisher's z-transformation is part of the method multiverse.

On a related note, the number of training data (selected points/-forking paths) can also be one important forking path for the method multiverse since the performance of the active learning model also depends on the selected training points. For an example, we performed a small analysis with two different scenarios to select 30 training points: (i) 5 points selected randomly and 25 points selected via Bayesian optimization and (ii) 30 points selected randomly. We found that after completing the training with 30 selected points, the Spearman correlations of the prediction performance of all the forking paths between the active learning and exhausting search are 0.48 and 0.58 for case (i) and case (ii) in ABCD dataset and 0.57 and 0.60 for case (i) and case (ii) for HCP dataset. For reference, the Spearman correlations from the original approach (10 points randomly selected and 20 points via Bayesian optimization) are 0.67 and 0.75 for ABCD and HCP datasets, respectively. The results suggest that variability of the outcomes may occur with different methods to select the learning points. Therefore, future studies may consider a more systematic multiverse analysis that considers the forking paths in the methodological steps, or the multiverse of the method (method multiverse). Moreover, the use of different behavioral measures to define a latent variable (e.g. g), or the multiverse of the

outcome variable (outcome multiverse), can also be explored.

Notably, there are steps/forking paths with a huge number of options (the one with continuous variables or the one with infinite discrete values) or with options that are mutually exclusive. In those cases, the number of forking paths exponentially grows and the implementation of multiverse analysis may not be computationally feasible. The approaches to define the garden of forking paths, or generally the question how to correctly and efficiently perform a multiverse analysis, are still being discussed. Del Giudice and Gangestad 2021, proposed that assessment of equivalence of the options/forking paths in terms of measurement, effect, and power/precision may help to reduce the number of forking paths. A sampling method across all the forking paths can also be conducted to reduce the number of forking paths (Paul et al. 2022).

Finally, the visualization application is still being improved, both visually and technically, e.g., by adding more features that allow users to interact more easily with the multiverse. Moreover, integrating the visualization app and the active learning approach into one toolbox will be an important contribution to studies on multiverse analysis. Especially, the implementation into a toolbox with graphical user interface (GUI) that can be generalized across different research domains will facilitate the application of multiverse analysis in different fields.

Conclusion

Guided multiverse analysis (Dafflon et al. 2022) is necessary in fields dealing with complex data structures, such as graph-theory fMRI based brain-behavior association research. Such associations are widely studied in computational psychiatry and neurocognitive psychology, where the behavioral variables of interest are inherently latent. Our extension of the guided multiverse analysis method (Dafflon et al. 2022) makes the approach suitable for a broader community interested in assessing the robustness of findings across a large number of possible analytical choices when predicting a latent variable with graph theory fMRI measures.

Acknowledgments

This work was supported by a grant from the German Research Foundation (DFG) to Andrea Hildebrandt (HI 1780/7-1), Carsten Gießing (GI 682/5-1), Stefan Debener (DE 779/8-1) and Christiane Thiel (TH 766/9-1) as part of the DFG priority program "META-REP: A Meta-scientific Programme to Analyse and Optimise Replicability in the Behavioural, Social, and Cognitive Sciences" (SPP 2317) and a fellowship awarded from the Hanse-Wissenschaftskolleg (Institute of Advanced Study) in Delmenhorst, Germany, and the School for Medicine and Health Sciences at the University of Oldenburg to Daniel Kristanto. Data used in the preparation of this article were obtained from the Adolescent Brain Cognitive Development (ABCD) Study <https://abcdstudy.org>, held in the NIMH Data Archive (NDA). This is a multisite, longitudinal study designed to recruit more than 10,000 children aged 9–10 and follow them over 10 years into early adulthood. The ABCD Study® is supported by the National Institutes of Health and additional federal partners under award numbers U01DA041048, U01DA050989, U01DA051016, U01DA041022, U01DA051018, U01DA051037, U01DA050987, U01DA041174, U01DA041106, U01DA041117, U01DA041028, U01DA041134, U01DA050988, U01DA051039, U01DA041156, U01DA041025, U01DA041120, U01DA051038, U01DA041148, U01DA041093, U01DA041089,

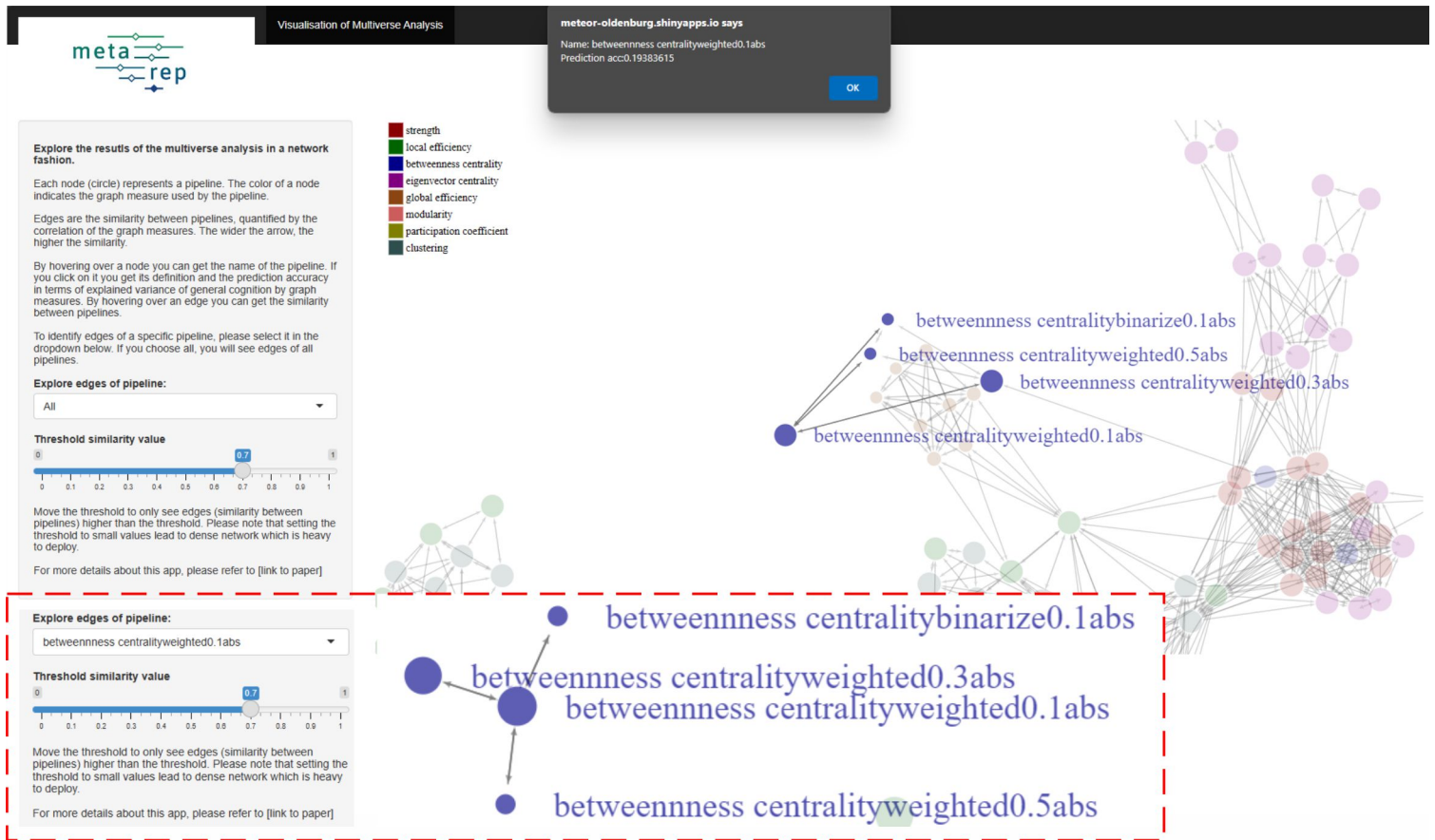


Figure 5: Screenshot of the interactive Shiny application for the visualization of the multiverse of analysis results. The multiverse is visualized as a network where the nodes are the forking paths and the edges indicate the similarity between the forking paths.

U24DAO41123, U24DAO41147. A full list of supporters is available at <https://abcdstudy.org/federal-partners.html>. A listing of participating sites and a complete listing of the study investigators can be found at https://abcdstudy.org/consortium_members/. ABCD consortium investigators designed and implemented the study and/or provided data, but did not necessarily participate in the analysis or writing of this report. This paper reflects the views of the authors and may not reflect the opinions or views of the NIH or ABCD consortium investigators. The ABCD data repository grows and changes over time. The ABCD data used in this report came from <https://doi.org/10.15154/1504041>.

Code and Data Availability

Codes to run the analysis of this study are available at <https://github.com/kristantodan12/ExtendedAL>. Computed graph measures, behavioral scores, and the list of pipeline for HCP dataset are available at <https://github.com/kristantodan12/ExtendedAL>, while for ABCD dataset are available at <https://nda.nih.gov/study.html?id=2428>.

Citation

Brainiacs 2023 Volume 4 Issue 2 Edoc J962E0F53

Title: "An Extended Active Learning Approach to Multiverse Analysis: Predictions of Latent Variables from Graph Theory Measures of the Human Connectome and Their Direct Replication"

Authors: Daniel Kristanto, Carsten Gießing, Merle Marek, Changsong Zhou, Stefan Debener, Christiane Thiel, Andrea Hildebrandt

Dates: received 2023-09-22, presented 2023-10-09, published 2023-12-21, endorsed 2023-12-30

Copyright: © 2023 Brain Health Alliance

Contact: [D Kristanto at Univ Oldenburg](mailto:D.Kristanto@univ-oldenburg.de)

URL: [Brainiacsjournal.org/arc/pub/Kristanto2023MVMRIA](https://brainiacsjournal.org/arc/pub/Kristanto2023MVMRIA)

PDP: [/Nexus/Brainiacs/Kristanto2023MVMRIA](https://nexus.brainiacs.org/Kristanto2023MVMRIA)

DOI: [10.48085/J962E0F53](https://doi.org/10.48085/J962E0F53)

References

- [1] M. Alavash, C. C. Hilgetag, C. M. Thiel, and C. Gießing. "Persistence and flexibility of complex brain networks underlie dual-task interference." *Human Brain Mapping* 36.9 (2015), pp. 3542–3562. DOI: [10.1002/hbm.22861](https://doi.org/10.1002/hbm.22861) (cited p. 2).
- [2] J. J. Allaire, C. Gandrud, K. Russell, and C. J. Yetman. *networkD3: D3 JavaScript Network Graphs from R*. 2022. URL: <https://cran.r-project.org/web/packages/networkD3/networkD3.pdf> (cited p. 5).
- [3] D. L. Barabási, G. Bianconi, E. Bullmore, M. Burgess, et al. "Neuroscience Needs Network Science." *Journal of Neuroscience* 43.34 (2023), pp. 5989–5995. ISSN: 15292401. DOI: [10.1523/JNEUROSCI.1014-23.2023](https://doi.org/10.1523/JNEUROSCI.1014-23.2023) (cited p. 2).
- [4] A. K. Barbey. "Network Neuroscience Theory of Human Intelligence." *Trends in Cognitive Sciences* 22.1 (2018), pp. 8–20. ISSN: 1879307X. DOI: [10.1016/j.tics.2017.10.001](https://doi.org/10.1016/j.tics.2017.10.001) (cited p. 2).
- [5] D. M. Barch, G. C. Burgess, M. P. Harms, S. E. Petersen, et al. "Function in the human connectome." *Neuroimage* 19 (2009), pp. 389–399. ISSN: 08966273. DOI: [10.1016/j.asieco.2008.09.006](https://doi.org/10.1016/j.asieco.2008.09.006). EAST (cited p. 3).
- [6] R. Botvinik-Nezer, F. Holzmeister, C. F. Camerer, A. Dreber, et al. "Variability in the analysis of a single neuroimaging dataset by many teams." *Nature* 582.7810 (2020), pp. 84–88. ISSN: 14764687. DOI: [10.1038/s41586-020-2314-9](https://doi.org/10.1038/s41586-020-2314-9) (cited pp. 1, 2, 5, 6).
- [7] O. J. Bruton. "Is there a 'g-neuron'? Establishing a systematic link between general intelligence (g) and the von Economo neuron." *Intelligence* 86.November 2020 (2021), p. 101540. ISSN: 01602896. DOI: [10.1016/j.inte11.2021.101540](https://doi.org/10.1016/j.inte11.2021.101540) (cited p. 2).
- [8] B. J. Casey, T. Cannonier, M. I. Conley, A. O. Cohen, et al. "The Adolescent Brain Cognitive Development (ABCD) study : Imaging acquisition across 21 sites." *Developmental Cognitive Neuroscience* 32.March (2018), pp. 43–54. ISSN: 1878-9293. DOI: [10.1016/j.dcn.2018.03.001](https://doi.org/10.1016/j.dcn.2018.03.001) (cited p. 3).
- [9] W. Chang, J. Cheng, J. J. Allaire, C. Sievert, et al. *shiny: Web Application Framework for R*. 2023. URL: <https://github.com/rstudio/shiny> (cited p. 5).
- [10] G. Chen, G. Chen, C. Xie, and S. J. Li. "Negative Functional Connectivity and Its Dependence on the Shortest Path Length of Positive Network in the Resting-State Human Brain." *Brain Connectivity* 1.3 (2011), pp. 195–206. ISSN: 21580022. DOI: [10.1089/brain.2011.0025](https://doi.org/10.1089/brain.2011.0025) (cited p. 5).
- [11] J. Chen, A. Tam, V. Kebets, C. Orban, et al. "Shared and unique brain network features predict cognitive, personality, and mental health scores in the ABCD study." *Nature Communications* 13.1 (2022). ISSN: 2041-1723. DOI: [10.1038/s41467-022-29766-8](https://doi.org/10.1038/s41467-022-29766-8) (cited p. 2).
- [12] J. Dafflon, P. F. Da Costa, F. Váša, R. P. Monti, et al. "A guided multiverse study of neuroimaging analyses." *Nature Communications* 13.1 (2022). ISSN: 20411723. DOI: [10.1038/s41467-022-31347-8](https://doi.org/10.1038/s41467-022-31347-8) (cited pp. 2, 3, 6, 7, 10).
- [13] M. Del Giudice and S. W. Gangestad. "A Traveler's Guide to the Multiverse: Promises, Pitfalls, and a Framework for the Evaluation of Analytic Decisions." *Advances in Methods and Practices in Psychological Science* 4.1 (2021). ISSN: 25152467. DOI: [10.1177/2515245920954925](https://doi.org/10.1177/2515245920954925) (cited p. 10).
- [14] B. Fischl, D. H. Salat, E. Busa, M. Albert, et al. "Whole brain segmentation: Automated labeling of neuroanatomical structures in the human brain." *Neuron* 33.3 (2002), pp. 341–355. ISSN: 08966273. DOI: [10.1016/S0896-6273\(02\)00569-X](https://doi.org/10.1016/S0896-6273(02)00569-X) (cited p. 2).
- [15] A. R. Franco. "Spatial Stability of Functional Networks : A Measure to Assess the Robustness of Graph-Theoretical Metrics to Spatial Errors Related to Brain Parcellation." 15.February (2022), pp. 1–18. DOI: [10.3389/fnins.2021.736524](https://doi.org/10.3389/fnins.2021.736524) (cited p. 5).
- [16] M. F. Glasser, T. S. Coalson, E. C. Robinson, C. D. Hacker, et al. "A multi-modal parcellation of human cerebral cortex." *Nature* (2016). ISSN: 14764687. DOI: [10.1038/nature18933](https://doi.org/10.1038/nature18933) (cited p. 2).
- [17] M. F. Glasser, S. N. Sotiropoulos, J. A. Wilson, T. S. Coalson, et al. "The minimal preprocessing pipelines for the Human Connectome Project." *NeuroImage* 80 (Oct. 2013), pp. 105–124. ISSN: 1053-8119. DOI: [10.1016/J.NEUROIMAGE.2013.04.127](https://doi.org/10.1016/J.NEUROIMAGE.2013.04.127) (cited p. 2).
- [18] K. Hilger, M. Fukushima, O. Sporns, and C. J. Fiebach. "Temporal stability of functional brain modules associated with human intelligence." *Human Brain Mapping* 41.2 (2020), pp. 362–372. DOI: [10.1002/hbm.24807](https://doi.org/10.1002/hbm.24807) (cited p. 6).
- [19] L. Hubert and P. Arabie. "Comparing partitions." *Journal of Classification* 2.1 (1985), pp. 193–218. ISSN: 1432-1343. DOI: [10.1007/BF01908075](https://doi.org/10.1007/BF01908075) (cited p. 6).

- [20] A. A. Igolkina and G. Meshcheryakov. "semopy: A Python Package for Structural Equation Modeling." *Structural Equation Modeling: A Multidisciplinary Journal* 27.6 (Nov. 2020), pp. 952–963. ISSN: 1070-5511. DOI: [10.1080/10705511.2019.1704289](https://doi.org/10.1080/10705511.2019.1704289) (cited p. 5).
- [21] R. E. Jung and R. J. Haier. "The Parieto-Frontal Integration Theory (P-FIT) of intelligence: Converging neuroimaging evidence." *Behavioral and Brain Sciences* 30.2 (2007), pp. 135–154. ISSN: 0140525X. DOI: [10.1017/S0140525X07001185](https://doi.org/10.1017/S0140525X07001185) (cited pp. 2, 6).
- [22] R. B. Kline. *Principles and Practice of Structural Equation Modeling, Fourth Edition*. Methodology in the social sciences. New York, NY, US: Guilford Publications, 2015. ISBN: 9781462523009 (cited p. 2).
- [23] K. Kovacs and A. R. Conway. "Process Overlap Theory: A Unified Account of the General Factor of Intelligence." *Psychological Inquiry* 27.3 (2016), pp. 151–177. ISSN: 1047840X. DOI: [10.1080/1047840X.2016.1153946](https://doi.org/10.1080/1047840X.2016.1153946) (cited p. 2).
- [24] K. Kriegbaum, N. Becker, and B. Spinath. "The relative importance of intelligence and motivation as predictors of school achievement: A meta-analysis." *Educational Research Review* 25. February (2018), pp. 120–148. ISSN: 1747938X. DOI: [10.1016/j.edurev.2018.10.001](https://doi.org/10.1016/j.edurev.2018.10.001) (cited p. 2).
- [25] D. Kristanto, A. Hildebrandt, W. Sommer, and C. Zhou. "Cognitive abilities are associated with specific conjunctions of structural and functional neural subnetworks." *NeuroImage* 279. November 2022 (2023), p. 120304. ISSN: 1053-8119. DOI: [10.1016/j.neuroimage.2023.120304](https://doi.org/10.1016/j.neuroimage.2023.120304) (cited p. 2).
- [26] G. Meshcheryakov, A. A. Igolkina, and M. G. Samsonova. "semopy 2: A structural equation modeling package with random effects in python." *arXiv preprint arXiv:2106.01140* (2021) (cited pp. 5, 10).
- [27] K. Paul, C. A. Short, A. Beauducel, H. P. Carsten, et al. "The methodology and dataset of the coscience eeg-personality project – a large-scale, multi-laboratory project grounded in cooperative forking paths analysis." *Personality Science* 3 (2022), pp. 1–26. DOI: [10.5964/ps.7177](https://doi.org/10.5964/ps.7177) (cited pp. 1, 10).
- [28] R Core Team. *R: A Language and Environment for Statistical Computing*. Vienna, Austria: R Foundation for Statistical Computing, 2021. URL: <https://www.r-project.org/> (cited p. 5).
- [29] M. Rubinov, R. Kötter, P. Hagmann, and O. Sporns. "Brain connectivity toolbox: a collection of complex network measurements and brain connectivity datasets." *NeuroImage* 47 (2009), S169. ISSN: 1053-8119. DOI: [https://doi.org/10.1016/S1053-8119\(09\)71822-1](https://doi.org/10.1016/S1053-8119(09)71822-1) (cited p. 5).
- [30] A. Schaefer, R. Kong, E. M. Gordon, T. O. Laumann, X.-N. Zuo, A. J. Holmes, S. B. Eickhoff, and B. T. T. Yeo. "Local-Global Parcellation of the Human Cerebral Cortex from Intrinsic Functional Connectivity MRI." *Cerebral Cortex* 28.9 (2018), pp. 3095–3114. ISSN: 1047-3211. DOI: [10.1093/cercor/bhx179](https://doi.org/10.1093/cercor/bhx179) (cited pp. 2, 6).
- [31] B. Settles. *Active Learning Literature Survey*. Tech. rep. 1648. 2009. URL: <https://research.cs.wisc.edu/techreports/2009/TR1648.pdf> (cited p. 2).
- [32] N. C. Silver and W. P. Dunlap. "Averaging correlation coefficients: Should Fisher's z transformation be used?" *Journal of Applied Psychology* 72.1 (1987), pp. 146–148. ISSN: 1939-1854(Electronic), 0021-9010(Print). DOI: [10.1037/0021-9010.72.1.146](https://doi.org/10.1037/0021-9010.72.1.146) (cited p. 5).
- [33] C. Spearman. ""General Intelligence" Objectively Determined and Measured." (1904) (cited p. 2).
- [34] S. Steegen, F. Tuerlinckx, A. Gelman, and W. Vanpaemel. "Increasing Transparency Through a Multiverse Analysis." *Perspectives on Psychological Science* 11.5 (2016), pp. 702–712. ISSN: 17456924. DOI: [10.1177/1745691616658637](https://doi.org/10.1177/1745691616658637) (cited p. 2).
- [35] R. L. Thorndike. "Who belongs in the family?" *Psychometrika* 18.4 (1953), pp. 267–276. ISSN: 1860-0980. DOI: [10.1007/BF02289263](https://doi.org/10.1007/BF02289263) (cited p. 6).
- [36] J. Xiang, J. Xue, H. Guo, D. Li, et al. "Graph-based network analysis of resting-state fMRI: test-retest reliability of binarized and weighted networks." *Brain Imaging and Behavior* 14.5 (2020), pp. 1361–1372. ISSN: 19317565. DOI: [10.1007/s11682-019-00042-6](https://doi.org/10.1007/s11682-019-00042-6) (cited p. 5).
- [37] B. T. Yeo, F. M. Krienen, J. Sepulcre, M. R. Sabuncu, et al. "The organization of the human cerebral cortex estimated by intrinsic functional connectivity." *Journal of Neurophysiology* 106.3 (2011), pp. 1125–1165. ISSN: 00223077. DOI: [10.1152/jn.00338.2011](https://doi.org/10.1152/jn.00338.2011) (cited p. 6).